

Macro parameters describing the mechanical behavior of classical guitars

Benjamin Elie^{a)} and François Gautier

LAUM, UMR CNRS 6613, Avenue Olivier Messiaen F-72085 Le Mans Cedex 9, France

Bertrand David

Institut Mines-Télécom, Télécom ParisTech, CNRS LTCI 46 rue Barrault F-75634 Paris Cedex 13, France

(Dated: September 30, 2012)

In reference papers dating back to the 60's and 70's, different authors proposed simplified models for the vibro-acoustical behavior of string instruments in the low-frequency range, using a few parameters. In this paper, a method is described which allows to derive and estimate a few salient parameters (or *features*) describing the mechanical behavior of classical guitars in a broader frequency range. These features are selected under the constraint that the measurements are easily realizable at the instrument maker workshop. The computations of these features rely on the estimation of the modal parameters over a large frequency range, thanks to the high-resolution subspace ESPRIT method, associated with the signal enumeration technique ESTER. The methods are here applied to numerical simulations and experiments on real metallic and wood plates. The results on guitars show a constant modal density in the mid and high-frequency domains as it would be for a flat panel. Finally, 4 features are chosen as characteristic parameters of this equivalent plate, namely the mass, rigidity, characteristic admittance and the mobility deviation. Applications on a population of guitars indicate that these features are good candidates to discriminate different classes of classical guitars.

PACS numbers: 43.75.Gh, 43.75.Yy

I. INTRODUCTION

In the 60's and 70's, Schelleng¹, Caldersmith², and Christensen³, proposed simple models for the low-frequency mechanical behavior of string instruments. These studies, while giving a better understanding of the role of important elements such as the rose for the guitar, also reduce the complexity of a whole system to a few simple substructures (2 coupled mass-string systems^{2,3} for the guitar soundboard-soundbox interaction, or an electric circuit¹ for the violin). This reduction mainly relies on a low-frequency assumption, which enables the modeling of mechanical and acoustical elements with the help of lumped equivalent circuits. For extending the study of complex vibrators to broader frequency ranges, where the concept of lumped circuits does not apply, statistical⁴ or finite elements methods^{5,6} have been thoroughly exploited. In this paper, we follow another approach, which consists to address the issue of designing and estimating a few parameters able to characterize an instrument in the mid and high-frequency ranges as well as in the low-frequency register. We particularly focus for the application of this approach to classical guitars.

In the low-frequency range, the mechanical behavior of weakly damped vibrating structures is usually described using eigenmodes. For higher frequency ranges, the spectral overlap of modes increases, often due to higher damping and sometimes higher modal density and the modal theory becomes ineffective^{4,7}. This is likely a ratio for

which authors have tried alternative approaches to capture the important and salient properties of a whole instrument: there is a need for summarizing its behavior along the whole frequency range with a few parameters (or features) and we expect them to discriminate instruments of the same kind.

For instance, a number of authors have investigated the vibro-acoustical properties by considering the radiation efficiency^{8,9}. Hill *et al.*¹⁰ designed a profile analysis of classical guitars with a method based on low-frequency input admittance and sound-pressure response. Earlier, Meyer and Janson¹¹ proposed a small set of selected features to be related to the quality of the guitar. Recently, Ege¹² has suggested describing globally the piano soundboard with a method based on modal density estimation. More generally, the salience of such features or macro-parameters is sometimes assessed with the help of subjective evaluation^{8,13-15}.

Hence, there are a number of solutions to deal with the issue of summarizing the vibro-acoustical behavior of a guitar in a few features. Since our work has been initiated from a collaboration with instrument makers and will be developed in the future in this framework, we only have considered the features which are computable from mechanical measurements made within a workshop context.

When a guitar string is plucked by the musician, its vibration is transmitted to the soundboard via the bridge. This makes the study of the string-soundboard coupling a good candidate for our purposes while the measurement of the mechanical admittance, also called mobility, is realizable in the workshop for interested makers. On plucked instruments, the level of that coupling acts on

^{a)}benjamin.elie.etu@univ-lemans.fr

both the sound level and the sound duration¹⁶: when it is strong (*i.e.* large mobility), the energy of the string is more suddenly transferred to the soundboard, resulting in a more powerful sound, but with faster decay. The trade-off between sound level and sound duration is a frequent issue to be tackled by instrument makers.

The main aspects of our approach are outlined by the organization of the paper. In Section II, we follow Langley¹⁷, Skudrzyk¹⁸, and Ege¹² to design useful and salient features from the measurement of bridge mobility. In order to estimate robustly these features, an original signal processing method, extending the modal identification to higher frequency ranges is presented in Section III. The performance of the method is studied in Section IV, using a test framework combining a controlled dataset with realistic noisy environment. The method is then used in experiments with real wood and metallic thin plates. These experiments lead us to apply confidently the method to guitar mobility measurements (Section V), making it possible to visualize guitars as points in a well chosen feature space.

II. DESCRIPTION OF BRIDGE MOBILITY USING A FEW PARAMETERS

In this paper, the experimental framework is restricted to that suitable from a daily instrument maker practice. Thus, the normal mobility is the only one considered for this study. This approximation restricts the possible degrees of freedom to the unique transverse motion, that is the translation perpendicular to the soundboard. When in the general case, the mobility would have been a matrix¹⁹, expressed in the frequency domain, here it becomes a simple scalar $Y(\omega)$ which amounts to the ratio between the transverse velocity in the Fourier domain $V(\omega)$ and the excitation force $F(\omega)$ in the same direction and at the same location. This mobility is usually measured at one of the points of the bridge where strings are attached.

Figure 1 shows typical mobility curves, measured at the bridge of two different guitars at the point where the E2 string is attached. Both plots of $|Y|$ as function of the frequency include numerous modal contributions and overall tendencies which results in different but rather complicated patterns and makes the comparison between the instruments not straightforward. In this section, we propose to consider a small set of quantities able to highlight the meaningful information comprised in $Y(\omega)$.

To this aim, the work of Skudrzyk on what he has called the characteristic admittance¹⁸ and that of Langley on the envelope curves of mobility¹⁷ have particularly been found useful. Both approaches allow a description of vibratory responses in the mid and high-frequency ranges and are adapted for the case of stringed instruments.

A. Modal Overlap Factor (MOF) and frequency ranges

It is usual to split the frequency response of mechanical systems into three domains: the low, mid and high-

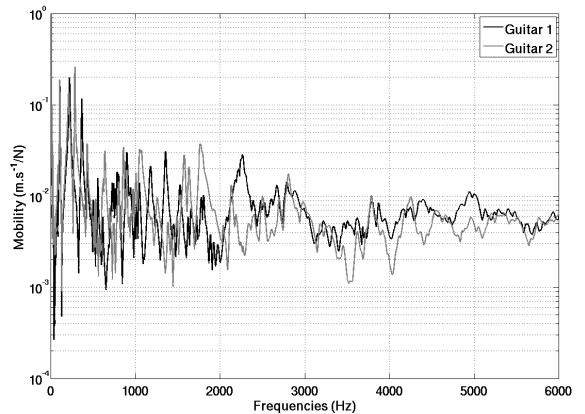


Figure 1. Modulus of the mobility plotted versus frequency, measured at the bridge of two different guitars.

frequency ranges. In the low-frequency range, the mobility shows resonances as well separated peaks, easy to segregate and identify. When higher frequencies are considered, the modal peaks tend to overlap largely because of higher damping in addition or not of greater modal density. The boundaries of these domains have been specified using the value of the *Modal Overlap Factor* or MOF⁵, defined as μ , the ratio of the half-power bandwidth to the frequency difference of two successive eigenmodes. More precisely, let ω_k be the center angular frequency of a resonance peak, ω_{k+1} the next modal center angular frequency and $\Delta\omega_k$ the half-power bandwidth, the MOF μ_k writes:

$$\mu_k = \frac{\Delta\omega_k}{\omega_{k+1} - \omega_k}, \quad (1)$$

The boundaries of the frequency ranges are commonly defined as follows⁵:

- low-frequency range : $\mu < 30\%$,
- mid-frequency range : $30\% < \mu < 100\%$,
- high-frequency range : $\mu > 100\%$.

From a practical point of view, μ is obtained as a function of frequency by averaging the μ_k 's over a sliding window containing a predefined number of modes (typically 11 modes).

B. Characteristic admittance

The so-called characteristic admittance Y_C of a finite structure is defined by Skudrzyk¹⁸ as the mobility of the equivalent structure with infinite dimensions. Skudrzyk¹⁸ derives a closed-form expression to estimate the real part of the characteristic admittance, $G_C = \Re(Y_C)$, of the finite structure from its properties:

$$G_C(\omega) = \frac{\pi n(\omega)}{2M_{Tot}}, \quad (2)$$

where $n(\omega)$ denotes the local modal density and M_{Tot} is the total mass of the system.

To obtain Equation (2), Skudrzyk's technique consists in changing the expression of the mechanical admittance from a discrete sum to an integral. However, the calculation of this integral is based upon several assumptions:

- the modal overlap is supposed to be large enough, so that the modal contributions are no longer individually observable,
- the structure is supposed to be homogeneous (the surface density is constant over the whole structure),
- the generalized damping matrix is supposed to be diagonal (Basile hypothesis),
- the modal loss factor is assumed to be constant over the whole frequency range.

The above hypotheses are in particular valid for plate-like systems, for which analytical expressions of modal density have been previously proposed²⁰⁻²³. The modal density of rectangular plates is known to tend asymptotically toward a constant, which has been estimated by Courant²⁰:

$$n_{\infty}(\omega) = \frac{S}{4\pi} \sqrt{\frac{\rho h}{D}}, \quad (3)$$

where S , h , and ρ denote respectively the surface, the thickness and the surface density of the plate, D being the flexural rigidity.

The substitution of Equation (3) in (2) leads to the expression of the asymptotic value of the characteristic admittance of rectangular flat panels:

$$G_{C_{\infty}} = \frac{1}{8\sqrt{\rho h D}}. \quad (4)$$

The value of $G_{C_{\infty}}$ can be used as an indicator to quantify the ability of the structure to vibrate, a structure with large characteristic admittance being globally more mobile, therefore more efficient to vibrate. The value will be expressed in dB, where the reference at 0 dB is the characteristic admittance of a 2-mm thick infinite plate having the typical mechanical properties of the spruce. Thus:

$$G_{C_{dB}} = 20 \log_{10} \left(\frac{G_{C_{\infty}}}{G_{Ref}} \right), \quad (5)$$

where G_{Ref} is the characteristic admittance computed from Equation 4, with $\rho = 420 \text{ kg.m}^{-3}$, $h = 2 \text{ mm}$, and $D = 2.1 \text{ N.m}$. Therefore, $G_{Ref} = 0.094 \text{ m.s}^{-1}.\text{N}^{-1}$.

In the case of conservative thin plates, the imaginary part of the mobility of an infinite plate is zero (*cf.* Ref.⁴, pages 34-39), therefore the imaginary part of the characteristic admittance is null.

C. Envelope curves of the mobility

The characteristic admittance is a relevant descriptor as it gives information about the mean-value of mobility. The scattering of the mobility around its mean-value can be described by the envelope curves, which represent the upper and lower bounds of the admittance modulus as a function of the frequency. For two structures having the same characteristic admittance, and the same modal density, their envelope curves will differ according to their loss factor. Langley¹⁷ gives an expression of envelope curves of mobility. Considering first the difference in frequencies between two successive resonances ω_k and ω_{k+1} evenly distributed and equal to the inverse of the local modal density $n(\omega)$, then considering that antiresonance frequencies between two successive resonances are $\omega = \frac{\omega_k + \omega_{k+1}}{2}$, the expression for the real part part of the mobility at resonances and antiresonances is written:

$$\begin{cases} G_{Res} = G_C \coth \left[\frac{\pi\mu}{\zeta} \right] \\ G_{Ares} = G_C \tanh \left[\frac{\pi\mu}{\zeta} \right] \end{cases}, \quad (6)$$

where $\zeta = 2$ for one-dimensional structures, and $\zeta = 4$ for two-dimensional structures (*cf.* Ref¹⁷).

The coupling between a string and the soundboard is strongly related to the value of the soundboard mobility at frequencies corresponding to the eigenfrequencies of the string¹⁶. Basically, a large value of the real part of the soundboard mobility, at the point coupling between the soundboard and the string, leads to a strongly damped string mode. Consequently, if the deviation of the soundboard mobility is large, the damping coefficients of string modes of successive notes also vary a lot. Therefore, if a guitar presents a large deviation of its frequency response curve around its mean value, one can think that its behavior is less homogeneous than another guitar having a small deviation of its frequency response. In order to quantify this deviation with simple quantities, the area between the upper and lower envelope curves, normalized by the mean value of the mobility is estimated. This parameter, called the *mobility deviation*, is denoted by $\langle \sigma_Y \rangle_{\omega_{30}}$, and can be written:

$$\langle \sigma_Y \rangle_{\omega_{30}} = \frac{1}{\omega_{max} - \omega_{30}} \int_{\omega_{30}}^{\omega_{max}} \frac{G_{Res} - G_{Ares}}{G_C} d\omega, \quad (7)$$

where ω_{max} is the upper bound of the frequency band used for the analysis of the mobility. The angular frequency ω_{30} corresponds to the lower bound of the mid-frequency range and is defined as the angular frequency for which the modal overlap factor is greater than 30%.

III. MODAL IDENTIFICATION USING HIGH-RESOLUTION TECHNIQUES

In practice, the computation of the characteristic admittance and envelope curves requires an estimation of modal parameters. In the low-frequency range, several

Fourier based modal identification techniques^{24,25} have been developed. In the mid and the high-frequency ranges, the modal overlap increases^{4,5} and these methods are no longer robust. Subspace methods like MUSIC²⁶ (*MUltiple Signal Classification*), Matrix Pencil²⁷, or ESPRIT²⁸ (*Estimation of Signal Parameters via Rotational Invariance Techniques*) are then interesting to consider and have already been successfully applied to vibration signals (*cf.* Le Carrou²⁹ for the harp, David³⁰, Badeau³¹, and Ege³² for thin plates and piano, and Laroche³³ for guitars). Indeed, these methods overcome the Fourier resolution limit and are then useful when modes are overlapping (because of this property they are often called *high-resolution*). In our work, ESPRIT is used since it is known to be one of the more robust.

A. Modal description of the mobility

The eigenmodes of a dissipative system are the solutions of the homogeneous equation:

$$\mathbf{M}\ddot{\mathbf{x}} + \mathbf{C}\dot{\mathbf{x}} + \mathbf{S}\mathbf{x} = \mathbf{0}, \quad (8)$$

where \mathbf{M} , \mathbf{C} , and \mathbf{S} are respectively the mass, the damping, and the stiffness matrices, of size $N \times N$, where N is the number of modes, and \mathbf{x} is the generalized coordinates vector of the displacement.

The eigenmodes (λ_k , Φ_k) of the dissipative systems are known to be complex³⁴. The mobility can then be developed on the basis of the complex modes as:

$$Y_A(\omega) = j\omega \sum_{k=1}^N \left\{ \frac{u_k^2(A)}{\alpha_k + j(\omega + \omega_k)} + \frac{\bar{u}_k^2(A)}{\alpha_k + j(\omega - \omega_k)} \right\}, \quad (9)$$

$$u_k^2(A) = \frac{\Phi_k^2(A)}{2j\omega_k m_k},$$

where A denotes the point of observation, ω_k , α_k , m_k and Φ_k are respectively the modal angular frequency, the modal damping factor, the modal mass and the modal shape associated to the k^{th} mode. \bar{u}_k denotes the complex conjugate of u_k , the complex modal amplitude of the k^{th} mode.

If the damping matrix is such that the mode shapes Φ_k are reals, then Equation (9) can be rewritten in the form:

$$Y_A(\omega) = j\omega \sum_{k=1}^N \frac{\Phi_k^2(A)}{m_k(\omega_k^2 + j\eta_k\omega_k\omega - \omega^2)}, \quad (10)$$

where η_k denotes the modal loss factor of k^{th} mode.

The computation of the parameters described in the previous section requires the knowledge of the modal parameters ω_k , α_k , Φ_k , and m_k . The measurement and the analysis of the mobility using suitable techniques enable the modal parameter estimation in a broad frequency range.

B. Modal identification technique

From Equation (9), it comes that the velocity response $s(A, t)$ to an impulse force is the inverse Fourier transform of $Y_A(\omega)$. To emphasize that $s(A, t)$ is real, it is written as a real part of a sum of complex damped sinusoids:

$$s(A, t) = \Re \left[\sum_{k=1}^K b_k(A) z_k^t \right], \quad (11)$$

where $b_k(A) = a_k(A)e^{j\varphi_k(A)}$ is the complex amplitude of the k -th mode, and $z_k = e^{-\alpha_k + j\omega_k}$ denotes the corresponding pole with angular frequency ω_k and damping factor α_k . K is the number of modes between $\omega = -\pi F_s$ and $\omega = \pi F_s$, where F_s is the sampling frequency ($K = 2N$), the poles with negative frequency being the conjugate of those with positive frequency. These parameters are related to that of Equation (9) by:

$$b_k(A) = \frac{\Phi_k^2(A)}{2m_k} [1 + j\eta_k/2] \quad \text{and} \quad \alpha_k = \frac{1}{2}\eta_k\omega_k. \quad (12)$$

The ESPRIT²⁸ algorithm estimates the signal parameters corresponding to the modal parameters of the K sinusoidal components embedded in the signal. As the other subspace high resolution methods (such as Matrix Pencil or MUSIC), it is based on the decomposition of the data vector space onto two orthogonal subspaces, the so-called signal and noise subspaces. The signal subspace \mathcal{S} is that spanned by the sinusoidal components, *i.e.*, the family of the Vandermonde vectors $\mathbf{v}_{k=1 \dots K}$, with $\mathbf{v}_k = e^{j\omega_k t - \alpha_k t}$. The noise signal \mathcal{N} is the orthogonal complement of \mathcal{S} , such as $\mathcal{S} \oplus \mathcal{N} = \mathcal{E}$ where \mathcal{E} is the vector space spanned by the data vector. A basis $\mathbf{W}(K)$ of \mathcal{S} is obtained by computing the Singular Value Decomposition (SVD) of the Hankel data matrix computed from the measured signal samples. The signal subspace verifies the so-called rotational invariance property: it remains invariant from a sample to the next. This remark leads to the following property:

$$\mathbf{W}_\uparrow(K) = \mathbf{W}_\downarrow(K)\mathbf{R}(K), \quad (13)$$

where $\mathbf{R}(K)$ is a $K \times K$ matrix the eigenvalues of which are the poles z_k . $\mathbf{W}_\downarrow(K)$ is the matrix $\mathbf{W}(K)$ where the last row has been deleted and $\mathbf{W}_\uparrow(K)$ is the matrix $\mathbf{W}(K)$ where the first row has been deleted. The estimation of the poles z_k is done by an Eigen Value Decomposition of $\mathbf{R}(K)$. The reader can refer to Appendix A for a detailed description of the ESPRIT algorithm.

C. Signal enumeration

An important issue when applying subspace methods to composite signals is the tuning of the modeling order K , which is usually unknown. Several methods have been proposed to estimate K : the maximum

likelihood³⁵ method and Information Theoretic Criteria (ITC)³⁶, which include the Akaike Information Criteria (AIC)³⁷, and the Maximum Description Length (MDL)³⁸. More recently, the ESTER (*ESTimation of Error*) criterion, based upon the assessment of the rotational invariance property that characterizes the signal subspace, has been designed by Badeau *et al.*³¹ and used by Ege³² in the context of real world mechanical experiments. We thus chose to apply this technique since it proves reliable and also for its straightforward implementation with the ESPRIT algorithm.

This criterion consists in appraising the rotational invariance property of the signal sub-space with the error function

$$\mathbf{E}(p) = \mathbf{W}_\uparrow(p) - \mathbf{W}_\downarrow(p)\mathbf{R}(p). \quad (14)$$

The authors then introduce the function \mathbf{J} :

$$\mathbf{J}(p) = \frac{1}{\|\mathbf{E}(p)\|_2^2}. \quad (15)$$

$\mathbf{J}(p)$ is computed for $p = 1, 2, \dots, p_{max}$, where $p_{max} > K$, K being the right number of components residing in the signal. When the order p equals to the right number of poles ($p = K$), the matrix $\mathbf{W}(K)$ verifies the rotational invariance property, and consequently $\|\mathbf{E}(p)\|_2^2$ becomes null. $\mathbf{E}(p)$ can also be zero for $p < K$ since the subspace is then spanned by p sinusoids. Practically, we will obtain large values of \mathbf{J} for $p \leq K$ and smaller ones for $p > K$, when the subspace spanned by $\mathbf{W}(p)$ includes noise components. Note that for impulse responses signal, which is real, the number of components K is twice the number of physical eigenmodes.

IV. ROBUSTNESS OF THE METHOD

This section proposes numerical and experimental testings of the ESPRIT method, in order to assess the performance and the robustness of the method.

A. Test on realistic numerical simulations

In this section, the method is applied to synthetic test signals, designed to simulate accurately real measurement conditions while providing a ground truth for the modal parameters. It then allows to control precisely the macro-parameters as the noise level, the distribution of the modal component along the frequency axis and the modal overlap on purpose to assess the performance of the method for different values of these macro-parameters. The design of the synthetic signal is first described, followed by the main step of the whole, practical, signal processing method.

1. Hybrid synthesis of the acceleration and the force signals

The synthetic signals are designed by mixing a thin plate modal superimposition and measured noise out-

comes obtained from typical vibro-acoustic sensor; hence the denomination "Hybrid". Simulated impulse responses of rectangular, simply supported thin plates are then computed by following the steps below:

Step 1: synthesis of the noiseless impulse response. The modal parameters of a simply-supported rectangular plate, obeying the Kirchhoff-Love³⁴ model, are given by :

$$\omega_{n,m} = \frac{\pi^2}{\sqrt{\rho h}} \sqrt{D_1 \frac{n^4}{L_x^4} + D_3 \frac{m^4}{L_y^4} + (D_2 + D_4) \frac{n^2 m^2}{L_x^2 L_y^2}}, \quad (16)$$

$$\Phi_{n,m}(x, y) = \sin\left(\frac{n\pi x}{L_x}\right) \sin\left(\frac{m\pi y}{L_y}\right), \quad (17)$$

$$m_{n,m} = \Phi_{n,m}^T \mathbf{M} \Phi_{n,m} = \int_S \rho_S \Phi_{n,m}^2(x, y) dS, \quad (18)$$

where n and m are positive integers, L_x and L_y are respectively the dimensions of the plate along x and y . The terms D_i , with $i = 1, \dots, 4$, denote the flexural rigidity of the material, ρ_S is the surface density, and S is the surface.

The noiseless impulse response signal $s(t)$ is computed as a sum of the modal responses, by substituting the Equations (16)-(18) in Equations (11) and (12).

Step 2 : synthesis of the force signal $f(t)$. To resemble a force signal as produced by a real hammer impact, a typical waveform is proposed. It is a composite time-function built on two half-gaussians leading to an asymmetrical bell-shape which rises faster than it decays. The synthetic waveform has been chosen in agreement with the observation of a large set of different measured signals.

Step 3 : synthesis of the noiseless acceleration signal $\gamma(t)$. The noiseless acceleration signal $\gamma(t)$ is computed by convolving the signal force by the impulse response of the synthetic plate, *e. g.* $\gamma = f * s$.

Step 4 : noisy synthetic signal. Numerous noise signals have been recorded from the sensors used for our experiments attached to non excited plates. A segment of these measurements is randomly extracted and added both on the synthetic force and acceleration signals.

2. Impulse response estimation

Step 1: prewhitening ESPRIT is based on the assumption of an additive white noise, hence the necessity of a signal prewhitening before applying the estimation algorithm. In practice, it is often not difficult to obtain

Table I. Mechanical parameters of the aluminum plate

| Parameter | Units | Values | Parameter | Units | Values |
|-----------|-------|--------|-----------|--------------------|--------|
| L_x | mm | 280.0 | ρ | kg.m ⁻¹ | 2700.0 |
| L_y | mm | 350.0 | E | GPa | 69 |
| h | mm | 2.5 | ν | | 0.3 |

Table II. Mechanical parameters of the spruce plate.

| Parameter | Units | Values | Parameter | Units | Values |
|-----------|--------------------|--------|-----------|-------|--------|
| L_y | mm | 500 | D_1 | N.m | 17.2 |
| L_x | mm | 190 | D_2 | N.m | 1.0 |
| h | mm | 2.5 | D_3 | N.m | 1.3 |
| ρ | kg.m ⁻¹ | 433 | D_4 | N.m | 3.6 |

a measured noise alone, e.g. the mechanical system being not excited, either from the acceleration or the force sensor. This noise is then modeled as an autoregressive process of order 10. The corresponding transfer function is denoted by $H = 1/A$ and the noise whitening step then consists in filtering the signals (acceleration or force) by the inverse filter A^{31} .

Step 2: deconvolution The impulse response is estimated following a deconvolution technique. Assuming the mechanical system to be linear, the problem writes:

$$f * s = \gamma \quad (19)$$

The technique consists in estimating an approximate, finite impulse response, inverse filter \hat{g} for f . The approximation is defined in the mean least square sense as:

$$\hat{g} = \underset{\hat{g}}{\operatorname{argmin}} \|\hat{g} * f - \delta\|_2^2 \quad (20)$$

we then obtain an estimate \hat{s} of s as :

$$\hat{s} = \hat{g} * \gamma, \quad (21)$$

3. Application of the method to simulated plates

Impulse responses of 9 simulated plates are computed, with intermediate parameters of modal density and loss factors. This leads to 9 data set, corresponding to 9 plates that are represented in a loss factor-modal density plane in Figure 2. For additional information, the contour lines of equal MOF -or isoMOF- are drawn (dashed lines). Two of these 9 simulated plates are a simulation of panels that are used for the experimental validation, which is presented in Section IV.B: an aluminum plate, with a low modal density and low damping, and a spruce plate, with a higher modal density and higher damping. The geometrical and mechanical parameters of both plates are summarized in Tables I and II.

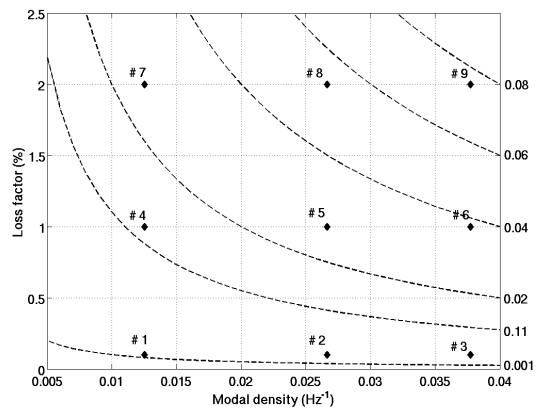


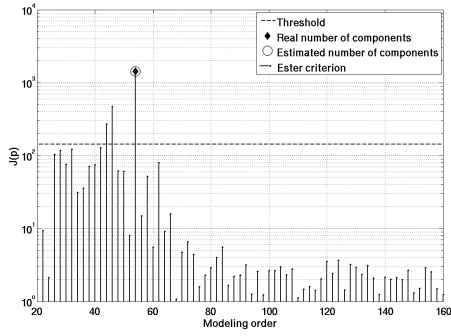
Figure 2. Modal density and loss factors of the 9 synthetic plates. The value of the modal density is computed from Equation (3). The "isoMOF" (dashed line) is the product of the modal density and loss factor values.

Following Section III.C, the modeling order (number of components of the impulse response) is selected as the integer K for which the ESTER criteria $J(p)$ remains below a certain threshold for $p > K$. Usually, $J(p)$ shows higher values in average for $p < K$ than for $p > K$ where it is often evenly lower. The threshold is set to a fraction of the global maximum, typically chosen as 1/10 or 2/5. Figure 3 shows the ESTER criterion applied to the plate #1 and the plate #6 .

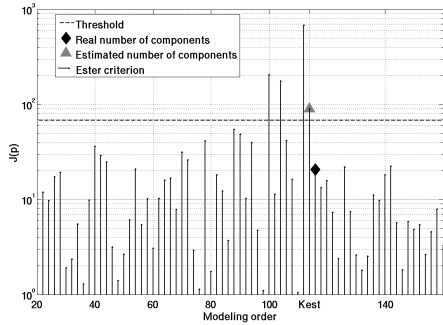
In practice, an overestimation of the number of modes often leads to unrealistic modal parameters (for instance a very high or negative damping). These aberrant values are easily discarded by a simple thresholding, consisting in rejecting modes estimated with negative damping or loss factors greater than an arbitrary threshold (set to 5% in our case).

In order to statistically assess the performance of the order estimation, 100 outcomes of simulated plate signals are computed. Each outcome uses a different noise segment following the scheme presented in Section IV.A.1. The performance of the method for the 9 synthetic plates is plotted in Figure 4, where error bars have been drawn, corresponding to the median absolute deviation.

For all plates, the number of components is accurately estimated. However, the estimation is rather dependent on the excitation and observation point. Indeed, if the excitation and observation points are in the vicinity of nodal lines, the corresponding modes are not detected by the method. This is especially the case when damping is large (e.g. plates #7 to 9), because the sinusoidal component is quickly drawn into noise, due to its large damping. Figure 4 confirms this tendency, since the number of components is rather underestimated, and the variation of estimation is higher when damping and/or modal density is large (i.e. the modal overlap is larger). However, the study focuses on the modal density of the guitar soundboard seen by the string. Thus, if the string applies a force in the vicinity of a mode node, it is not of great interest to detect it since that mode won't be excited.



(a)



(b)

Figure 3. (a) ESTER criterion, given by Equation (15), for the plate #1 versus the modeling order. The estimated modeling order in that case is 54, which matches the right number of components (54). (b) Results of the method applied to the plate #6. The estimated modeling order in that case is 114, which is slightly under the right number of components (116).

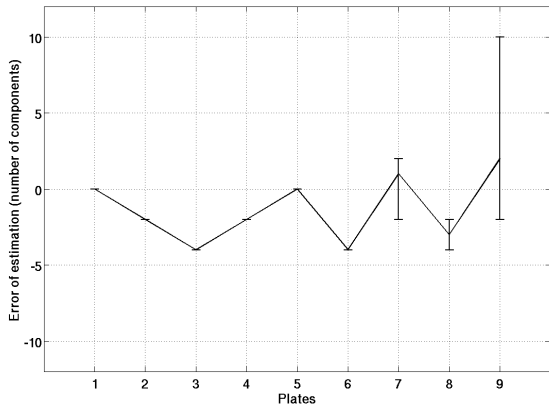


Figure 4. Comparison between the estimated number of components K_{est} and the real number of components K_{real} in the synthetic impulse response of the 9 plates. The values are the median and the median absolute deviation of a set of 100 realizations.

Besides, the study focuses on global parameters, a local error in the modal estimation is unlikely to be really influent on the final estimation of the global features.

B. Application to real plates

This section reports an experimental study using a rectangular aluminum plate and a rectangular spruce plate. The mechanical parameters of the tested plates are those given in Tables I and II.

1. Measurement set-up

The plates are hung with wires, fixed to its upper corners. This experimental set-up is intended to approach free-edge boundary conditions, while minimizing the added dissipation due to suspensions. The impulse response $s(t)$ is obtained by a synchronous and co-localized measurement of the excitation signal, using a small impact hammer (PCB 086E80), and the acceleration signal, by means of a small accelerometer (PCB 352C23, 0.2g). The plate is impacted at the same point than the measurement and the signal $s(t)$ is analyzed with the help of the ESPRIT method as described in Section III.B. The algorithm gives in output the estimated signal parameters Θ_k (the modal parameters, frequency, damping, amplitude, and phase). As discussed in Section II.A, the modal overlap factor, as well as the modal density, and the modal damping are averaged by means of a sliding window (in this study 11 consecutive modes are averaged). Finally, the global parameters defined in Section II (namely G_C , and the envelope curves) are computed from the values of the modal parameters.

2. Analysis of plate measurements

Figure 5 represents the ESTER criterion applied on the measured impulse response of both plates.

The overall spread of the ESTER criterion from measured data resembles those obtained in Section IV.A.3 with simulated data. This leads to apply confidently the method to estimate the number of components. Figure 6 shows the modal density, estimated by ESPRIT for the aluminum and spruce plates, computed from the ESPRIT-estimated modal frequencies and using Equation (22).

For both plates, the estimated modal density is found roughly constant, amounting to a value of 0.015 Hz^{-1} for the aluminum plate, and 0.0255 Hz^{-1} for the spruce plate. This results is in good agreement with the theoretical modal density of thin plates, known to be asymptotically constant. A close form of the asymptotic modal density, independently of the boundary conditions, has been derived by Courant²⁰ for isotropic plates. Recently, Xie *et al.*²¹ have proposed to add a corrective term, depending on the boundary conditions (*cf.* section V.B for details). The analytical modal density of free plates, after Xie²¹, is given by:

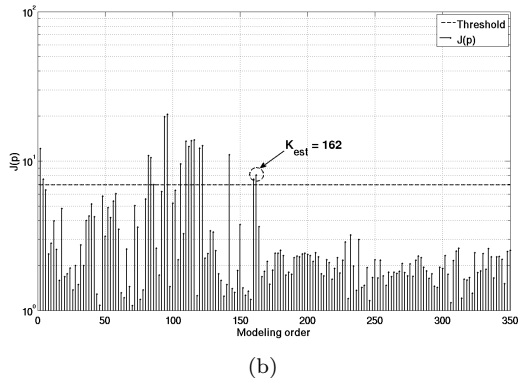
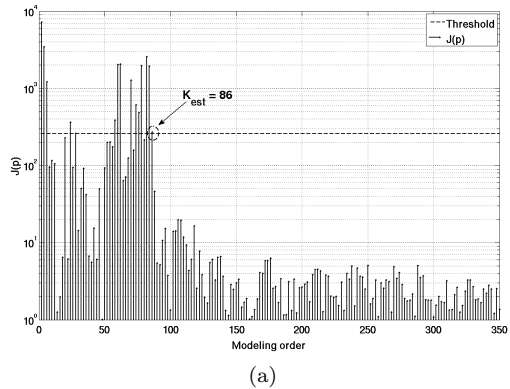


Figure 5. ESTER criterion for (a) the aluminum plate, and (b) the spruce plate.

$$n(\omega) = n_{\infty} + \frac{L_x + L_y}{2\pi} \left(\frac{\rho h}{D} \right)^{\frac{1}{4}} \omega^{-\frac{1}{2}}, \quad (22)$$

where n_{∞} is the asymptotic modal density given by Equation (3). The dashed line in Figure 5 represents the analytical modal density, after Equation (22). For the spruce plate, the analytical modal density is computed with the typical mechanical parameters of the spruce. The modal density estimated by ESPRIT from experimental data is in good agreement with that computed from Equation (22), showing that the number of modes estimated by ESTER is accurate.

V. APPLICATION TO GUITARS

A. Analysis of measured bridge mobility

For experimental testing, guitars are hanged by their headstock. The bridge mobility is measured using an accelerometer placed on the bridge, at the base of the E2 string, and a force hammer impacting at the same point. The present study focuses on the mechanical response of the guitar's soundboard at one string attachment point. The mean mobility level varies along the bridge: the bridge at the central strings (D3 and G3) attachment point is globally less mobile than at other string's attachment points.

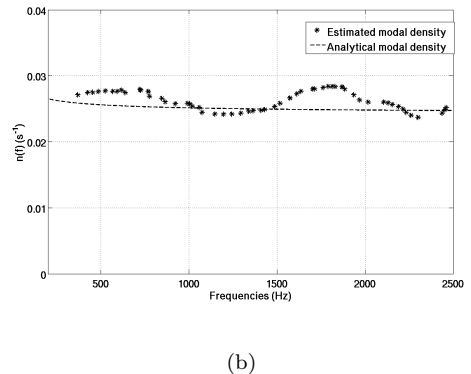
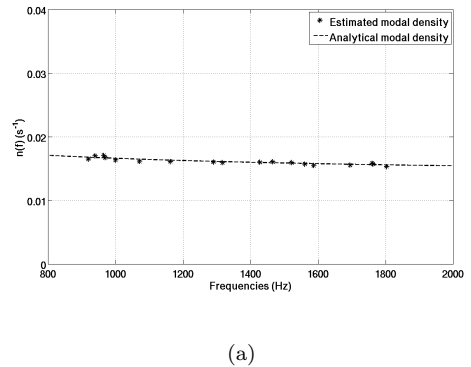
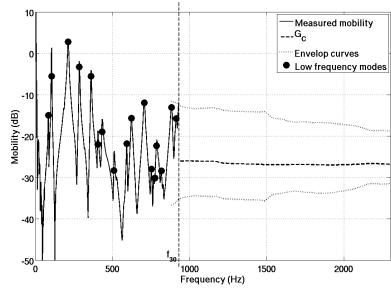


Figure 6. Modal density estimated by ESPRIT of (a) the aluminum plate, and (b) the spruce plate. The dashed line represents the analytical modal density after Equation 22 and Table III, when the boundary conditions are free. For the spruce plate, the analytical modal density is computed according to the typical values of the spruce, displayed in Table II.

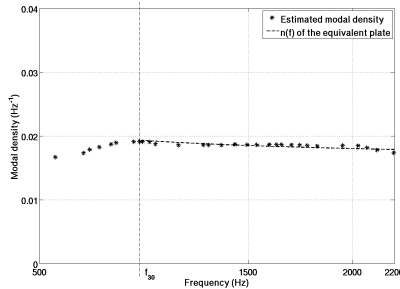
Figure 7 is an overall description of the mobility measured at the bridge of a guitar. The behavior of G_C , computed from Equation (2), in the mid and high-frequency ranges is typical of thin plates. This result suggests that guitars can be assimilated to an equivalent flat panel in these frequency domains. Furthermore, the computation of G_C highlights the global differences between instruments. This is one of the main results of this paper. The interest of such a result for the characterization of guitars is to reduce their characteristics to those of a rectangular thin plate that is equivalent to the guitar. The dashed line is the analytical modal density of the so-called equivalent plate. The modal damping is represented in Figure 7 (c). The modal loss factor is set between 1 and 2%, which is a typical value for wood materials, such as spruce^{39,40}.

B. Parameters of characterization: bending stiffness and mass

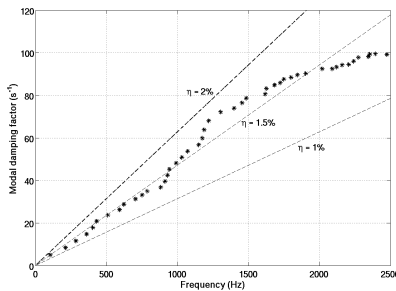
The analysis of the modal density of several guitars shows that it is roughly constant in the mid and the high-frequency ranges, which is a common feature of flat panels. We propose to determine the bending stiffness



(a)



(b)



(c)

Figure 7. (a) Overall representation of the mobility measured at the bridge of a guitar. (b) modal density and (c) modal damping factor estimated by ESPRIT and corresponding modal loss factors (dashed lines).

and the mass of the plate having the same modal density, *i.e.* the equivalent plate. This equivalent plate contains the contribution of every subsystem composing the whole instrument, namely the soundboard, the bridge, the bars, the back plate, the soundbox and so on. The method does not require prior information about the instrument. Although the materials used in instrument making are mainly orthotropic, the chosen model is an isotropic plate. The knowledge of the different rigidity moduli D_i is not necessary, and it is more convenient to estimate a global bending stiffness corresponding to the rigidity of the equivalent isotropic plate.

The modal density of plates writes:

$$n(\omega) = p\beta + q\sqrt{\beta/\omega}, \quad (23)$$

where $p = \frac{S}{4\pi}$, q is a constant coefficient depending on the boundary conditions and on the perimeter of the plate,

Table III. Parameter q for different boundary conditions

| Boundary conditions | q |
|---------------------|------------------------|
| free | $L_x + L_y$ |
| simply supported | $-\frac{L_x + L_y}{2}$ |
| clamped | $-(L_x + L_y)$ |

and $\beta = \sqrt{\frac{\rho h}{D}}$ is called the *plate elastic constant*, depending on the mechanical properties of the material. Table III gives the parameter q for different boundary conditions, according to Xie *et al.*²¹.

The plate elastic constant is determined by searching the value of β which minimizes the quadratic difference between the measured modal density and the model given by Equation (23). Hence:

$$\beta = \underset{\beta}{\operatorname{argmin}} \left\| \mathbf{n}_{30} - p\beta + q\sqrt{\beta}\mathbf{g}_{30} \right\|_2^2, \quad (24)$$

where $\mathbf{n}_{30} \in \mathbb{R}_+^{*\tilde{N}}$ is a vector containing the \tilde{N} measured values of the modal density at angular frequencies larger than ω_{30} , *i.e.* $\mathbf{n}_{30} = [n_j \ n_{j+1} \ \dots \ n_N]^T$, where j is the first mode order for which the modal overlap is higher than 30%, N being the number of modes estimated in the impulse response. The vector $\mathbf{g}_{30} \in \mathbb{R}_+^{*\tilde{N}}$ is the vector containing the \tilde{N} square root of the inverse measured modal angular frequencies in the mid-frequency range, *i.e.* $\mathbf{g}_{30} = [\omega_j^{-1/2} \ \omega_{j+1}^{-1/2} \ \dots \ \omega_N^{-1/2}]^T$. Considering $\beta \in \mathbb{R}_+^*$, Equation (24) has only one solution.

The estimation of the modal density for every guitar shows a slightly decreasing modal density in the mid-frequency range, which is proper to a freely vibrating plate. Consequently, the parameter q used for the study is the one corresponding to a plate with free boundary conditions.

Since the dimensions of classical guitars are very similar from a guitar to the next, those of the equivalent plate are set to the same value for each of them. The choice of the dimensions L_x and L_y is arbitrary. We chose to set these dimensions to those of a square plate with $L_x = L_y = 0.3$ m, since it roughly corresponds to the dimensions of the lower bout of the soundboard, which is the most mobile part. The values of parameters p and q in Equation (24) are $p = 7.2 \times 10^{-3}$ m² and $q = 0.6$ m.

The equivalent mass should be estimated by computing the spatial average of the modal amplitudes. In practice, this spatial average is delicate to achieve, because of the high number of required measurements.

We propose to estimate the equivalent mass from Equation (2). According to Skudrzyk, the characteristic admittance is the mean-line of the logarithmically plotted mobility curve; it is the geometrical mean between

a resonance and its successive antiresonance. It can be estimated by computing the moving average of the mobility curve, in dB. It consists in computing the mean value of the mobility, in dB, included in a sliding window of a certain span, this latter moving from a sample to the next. The obtained smoothed mobility $G_{smooth_{dB}}$ writes:

$$G_{smooth_{dB}}(\omega_c) = \frac{1}{\Delta\omega} \int_{\omega_1}^{\omega_2} Y_{dB} d\omega, \quad (25)$$

where $\Delta\omega = \omega_2 - \omega_1$, $\omega_c = \frac{\omega_1 + \omega_2}{2}$, ω_1 and ω_2 being respectively the lower and upper frequency bounds of the sliding window.

The equivalent mass is estimated from Equation (2), by means of the mean least squares method.

$$M = \frac{\pi}{2} \mathbf{n}_{fit} \cdot \mathbf{G}_{smooth_{dB}}^\dagger, \quad (26)$$

where \dagger denotes the Moore-Penrose pseudo-inverse, \mathbf{n}_{fit} is the analytical modal density of the equivalent plate, computed from Equation (23), and $\mathbf{G}_{smooth_{dB}}$ is the estimation of characteristic admittance G_C computed from Equation (25).

Tests on synthetic plates showed that the frequency span of the sliding window should be large (around 2000 Hz) in order to minimize the error of estimation on the equivalent mass.

Dividing the equivalent mass M_{Eq} by S gives the surface density ρh . Then, the equivalent bending stiffness is given by:

$$D_{Eq} = \frac{\rho h}{\beta^2}. \quad (27)$$

This method of characterization is not only dedicated to musical applications, but it applies to any plate-like structures and is relevant for estimating their characteristic parameters.

C. Results

Two groups of guitars have been studied. The first group is composed by 9 recent guitars made by instrument makers, considered as high quality instruments. They come from several different manufacturers and were lent by the store *La Guitarreria*, located in Paris. The second group is composed by industrial guitars of lower quality. The limits of the low-frequency domain, given by f_{30} , corresponding to the frequency from which the modal overlap factor is greater than 30% is given in Table IV.

1. Characteristic admittance vs. mobility deviation

A classification of the studied instruments is proposed by comparing the values of their characteristic admittance, denoted by $G_{C\infty}$, and their mobility deviation,

Table IV. Values of f_{30} for different studied guitars

| | 1 | 2 | 3 | 4 | 5 | 6 | 7 | 8 | 9 |
|-----------------------|-----|-----|-----|-----|-----|-----|-----|-----|-----|
| Group 1 f_{30} (Hz) | 772 | 910 | 834 | 465 | 767 | 835 | 754 | 603 | 850 |
| Group 2 f_{30} (Hz) | 506 | 602 | 635 | | | | | | |

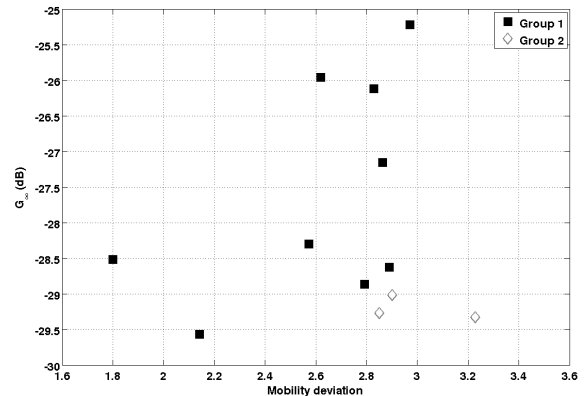


Figure 8. Classification of 2 groups of classical guitars by the values of their characteristic admittance $G_{C\infty}$ and their deviation of mobility

denoted by $\langle\sigma_Y\rangle$. The instruments can be represented in a plane defined by the values of $G_{C\infty}$ and $\langle\sigma_Y\rangle$, as shown in Figure 8.

Except in a few cases, the characteristic admittance of industrial guitars (group 2) is smaller than the one of hand-made guitars (group 1). Typically, the difference is from 1 up to 4 dB. Guitars from group 1 are therefore generally more efficient to vibrate.

The mobility deviation alone, however, is unlikely to discriminate the two groups: a large part of guitars from group 1 presents a mobility deviation in the same range than guitars from group 2, between 2.8 and 2.9. Nevertheless, some guitars from group 1 have a smaller mobility deviation, around 1.8 and 2.8.

2. Bending stiffness vs. equivalent mass

A classification of instruments is proposed by comparing the values of the mechanical properties of their equivalent plate, namely the bending stiffness D_{Eq} and the mass M_{Eq} . Figure 9 represents the position of the guitars in the plane defined by these two macro-parameters. The isomobility contour lines in Figure 9 represent the values of $G_{C\infty}$ corresponding to the values of D_{Eq} and M_{Eq} , after Equation (4).

The pair of parameters, equivalent mass and bending stiffness, when associated, is discriminant: the separation between the industrial guitars and the guitars from

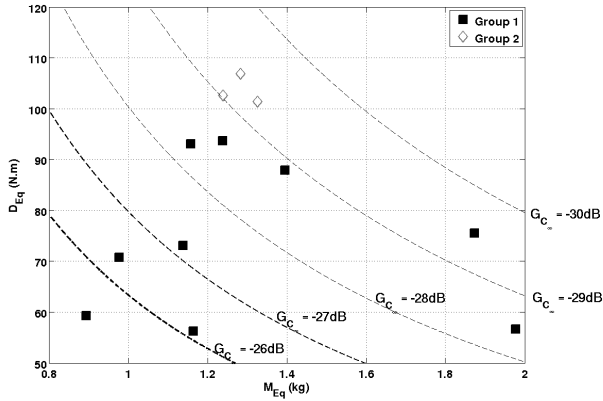


Figure 9. Classification of instruments by the values of the mechanical parameters of their equivalent plate (bending stiffness and mass). The isomobility contour lines (–) are given by dashed lines.

luthiers is straightforward. The industrial guitars present a high equivalent bending stiffness in comparison with those of guitars from group 1. However, the equivalent mass of industrial guitars is rather similar to those made by luthiers. The stiffness disparities between guitar groups can be explained by the nature of materials used for manufacturing. Indeed, industrial guitars are usually made with plywood, which is stiffer than solid woods (spruce or red cedar) used for soundboard manufacturing of high quality guitars.

It is worth noting that industrial guitars present similar properties, they tend to group together in the planes of both Figure 8 and Figure 9. This is certainly a consequence of the reproducible aspect of the industrial manufacturing process.

VI. CONCLUSIONS

The developed approach for this study enables the identification of modal density of structures. In spite of the fact that frequency responses of mechanical structures show high modal overlap, so that the modal parameters are difficult to identify by classical methods, the modeling of the impulse response of a structure as a sum of complex damped sinusoids, made up of the temporal responses of the mechanical modes, enables the ESPRIT method to estimate them with good precision, when associated with the signal enumeration technique ESTER.

Numerical and experimental validations on metallic and wood plates confirmed the accuracy of the method. Then, applications on guitars showed a common feature of their average mobility, this latter presenting a plate-like behavior in the mid-frequency domain. Thus, the guitar soundboard can be considered as a plate for frequencies higher than 800 Hz. From the values of modal parameters estimated by ESPRIT and some geometrical assumptions, it is possible to determine the mechanical properties of an equivalent plate (bending stiffness and

equivalent mass), allowing a simple characterization of guitars using only 4 scalar features, which are the equivalent mass and equivalent bending stiffness, the characteristic admittance of the equivalent plate, and the mobility deviation.

Applications on different populations of guitars highlight differences between instruments, especially in terms of average mobility, where the industrial guitars tend to have an average mobility smaller than guitars made by luthiers.

The difference in average mobility is attributed to the fact that industrial guitars, made with plywood, are stiffer than hand-made guitars, that present solid top of spruce or red cedar. The equivalent masses of all guitars are rather similar. It seems that one part of the luthier's savoir-faire consists in adjusting the global flexibility of the soundboard, so that they can control the mobility level. However, a high mobility is not necessarily a desirable quantity, as it can induce damped notes if this latter is very large at a particular frequency. The trade-off between powerful sound and sound duration is another role of the luthier. The homogeneity of mobility level with the frequency is assessed by the mobility deviation feature.

The mobility deviation feature, quantifying the scattering of the mobility around its mean-value, shows that, except in a few cases, all guitars present similar deviation of mobility around its mean-value.

Finally, the studied features seem to be good candidates to discriminate objectively instruments of the same kind, enabling eventually an instrument clustering. The application of the method shall be helpful for the instrument makers regarding the problematics encountered. They will dispose measurement tools enabling them to characterize objectively the mechanical behavior of their instrument with a set of few features.

Appendix A: ESPRIT ALGORITHM

Let $\mathbf{s} \in \mathbb{C}^N$ be the column vector of the measured signal, \mathbf{s} is a sum of K exponentially damped complex sinusoids corrupted by an additive white noise ε which the variance is σ^2 , hence:

$$s[n] = \sum_{k=1}^K b_k z_k^n + \varepsilon[n], \quad (\text{A1})$$

where b_k are the complex amplitudes of the sinusoids, and $z_k = e^{j\omega'_k - \alpha'_k}$ are the complex poles, $\omega'_k \in [-\pi, \pi]$ being the normalized angular frequency and $\alpha'_k \in \mathbb{R}_+$ being the normalized damping factor. The autocovariance matrix \mathbf{X} writes:

$$\mathbf{X} = \mathbb{E}[\mathbf{s}\mathbf{s}^H] \quad (\text{A2})$$

$$= \mathbf{V}\mathbf{B}\mathbf{V}^H + \sigma^2\mathbf{I}, \quad (\text{A3})$$

where \mathbb{E} and \cdot^H denote respectively the statistical expectation and the conjugate transpose of the matrix/vector, \mathbf{I} is the identity matrix, and $\mathbf{B} = \mathbf{b}\mathbf{b}^H$, \mathbf{b}

being the vector containing the complex amplitudes b_k :

$$\mathbf{b} = [b_1 \quad b_2 \quad \dots \quad b_K]^T. \quad (\text{A4})$$

The matrix $\mathbf{V} \in \mathbb{C}^{N \times K}$ is a base of the signal subspace \mathcal{S} spanned by the K complex sinusoids. It is a Vandermonde matrix containing the Vandermonde vectors $\mathbf{v}_k \in \mathbb{C}^N = [1 \quad z_k^1 \quad z_k^2 \quad \dots \quad z_k^N]^T$ of each individual sinusoid. The matrix \mathbf{V} writes:

$$\mathbf{V} = \begin{bmatrix} 1 & 1 & \dots & 1 \\ z_1 & z_2 & \dots & z_K \\ z_1^2 & z_2^2 & \dots & z_K^2 \\ \vdots & \vdots & \ddots & \vdots \\ z_1^{N-1} & z_2^{N-1} & \dots & z_K^{N-1} \end{bmatrix}. \quad (\text{A5})$$

The noise subspace \mathcal{N} is then the orthogonal complement of the signal subspace \mathcal{S} such as $\mathcal{S} \oplus \mathcal{N} = \mathcal{E}_N$, where \mathcal{E}_N is the vector space spanned by the N -dimensional data vector \mathbf{s} .

The signal subspace \mathcal{S} is characterized by the so-called rotational invariance (its base remains invariant from a sample to the next), which can be written into a matricial form:

$$\mathbf{V}_\uparrow = \mathbf{V}_\downarrow \mathbf{D}, \quad (\text{A6})$$

where \mathbf{V}_\uparrow is the matrix \mathbf{V} to which the first line has been withdrawn, and \mathbf{V}_\downarrow is the matrix \mathbf{V} to which the last line has been withdrawn. The matrix $\mathbf{D} \in \mathbb{C}^{K \times K}$ is a diagonal matrix, where the diagonal elements are the K poles of the signal :

$$\mathbf{D} = \text{diag}(z_1, \dots, z_K).$$

In practice, \mathbf{V} cannot be estimated, but a base of the signal subspace \mathcal{S} can be approached from a singular value decomposition (SVD) of the autocovariance matrix $\mathbf{X} = \frac{1}{r} \mathbf{H} \mathbf{H}^H$, where \mathbf{H} is a $l \times r$ Hankel matrix, with $r > K$ and $l = N + 1 - r > K$ is the sum of the dimensions of the signal and noise subspaces, composed by the measured signal samples:

$$\mathbf{X} = \mathbf{U} \mathbf{\Sigma} \mathbf{Z}, \quad (\text{A7})$$

where $\mathbf{U} \in \mathbb{C}^{l \times l}$ is a $l \times l$ matrix containing the l singular vectors $\{\mathbf{u}_1, \dots, \mathbf{u}_l\}$ associated to the l singular vectors sorted in decreasing order. The matrix $\mathbf{\Sigma} \in \mathbb{C}^{l \times l}$ is a diagonal matrix containing the l singular values $\{\lambda_1 \geq \lambda_2 \geq \dots \geq \lambda_l\}$ sorted in decreasing order. A base \mathbf{W} of \mathcal{S} can be approached by the concatenation of the K first singular vectors associated to the K larger singular values. The singular values from λ_{K+1} to λ_l are associated to the noise subspace \mathcal{N} . The base \mathbf{W} verifies the rotational invariance, hence:

$$\mathbf{W}_\uparrow(K) = \mathbf{W}_\downarrow(K) \mathbf{R}(K), \quad (\text{A8})$$

where $\mathbf{R} \in \mathbb{C}^{K \times K}$ is a $K \times K$ matrix which the eigenvalues are the poles of the signal. The poles z_k are then obtained by means of an eigenvalue decomposition of the matrix \mathbf{R} .

Finally, the steps for finding the complex poles are the following ones:

- compute the autocovariance matrix $\mathbf{X} = \frac{1}{r} \mathbf{H} \mathbf{H}^H$ where \mathbf{H} is the $l \times r$ Hankel matrix with the samples of the measured signal. The dimension l should be chosen such that $l > K$,
- compute $\mathbf{W}(K)$ by a concatenation of the K singular vectors associated to the K largest singular values from the SVD of \mathbf{X} ,
- compute $\mathbf{R}(K) = \mathbf{W}_\downarrow(K)^\dagger \mathbf{W}_\uparrow(K)$, where the symbol \dagger denotes the Moore-Penrose pseudo-inverse,
- extract the poles z_k as the eigenvalues of $\mathbf{R}(K)$.

ACKNOWLEDGMENTS

The authors would like to acknowledge the *Agence Nationale pour la Recherche* for the financial support of projet PAFI (*Plateforme d'Aide à la Fabrication Instrumentale*). We would also like to thank *La Guitarreria*, and the ITEM (Institut Technologique Européen des Métiers de la Musique) for the loan of instruments.

- ¹ J. C. Schelleng, "The violin as a circuit", *J. Acoust. Soc. Am.* **35**(3), 326–338 (1963).
- ² G. W. Caldersmith, "Guitar as a reflex enclosure", *J. Acoust. Soc. Am.* **63**(5), 1566–1575 (1978).
- ³ O. Christensen and B. B. Vistisen, "Simple model for low-frequency guitar function", *J. Acoust. Soc. Am.* **68**(3), 758–766 (1980).
- ⁴ R. H. Lyon, R. D. Dejong, *Theory and Application of Statistical Energy Analysis, second edition* (Butterworth Heinemann, Boston, 1995), Chap. 6.
- ⁵ J. Berthaut, M. N. Ichchou, and L. Jézéquel, "Piano soundboard: Structural behavior, numerical and experimental study in the modal range", *Appl. Acoust.* **64**, 1113–1136 (2003).
- ⁶ E. Bécache, A. Chaigne, G. Dervaux, and P. Joly, "Numerical simulation of a guitar", *Comput. Struct.* **83**, 107–126 (2005).
- ⁷ R. S. Langley, "A wave intensity technique for the analysis of high frequency vibrations", *J. Sound Vib.* **159**(3), 483–502 (1991).
- ⁸ F. Orduna-Bustamante, F. F. del Castillo Gomez, E. E. M. Montejo, and H. C. Tello, "Subjective and physical experiments related to the tuning of classical guitars.", *J. Acoust. Soc. Am.* **128**(4), 2447–2447 (2010).
- ⁹ J. C. S. Lai and M. A. Burgess, "Radiation efficiency of acoustic guitars", *J. Acoust. Soc. Am.* **88**(3), 1222–1227 (1990).
- ¹⁰ T. J. W. Hill, B. E. Richardson, and S. J. Richardson, "Acoustical parameters for the characterisation of the classical guitar", *Acta. Acust. Acust.* **90**, 335–348 (2004).
- ¹¹ J. Meyer, "Quality aspects of the guitar tone", in *Function, Construction and Quality of the Guitar*, edited by E. V. Jansson (Royal Swedish Academy of Music, Stockholm, Sweden, 1983), pp. 51–75.

- ¹² K. Ege and X. Boutillon, “Synthetic description of the piano soundboard mechanical mobility”, in *Proceedings of 20th International Symposium on Music Acoustics, Sydney and Katoomba, Australia*, 93–99, (2010).
- ¹³ F. Orduna-Bustamante and R. R. Boullosa, “Subjective evaluation of classical guitars”, *J. Acoust. Soc. Am.* **102**(5), 3086–3086 (1997).
- ¹⁴ R. R. Boullosa, F. Orduna-Bustamante, and A. P. Lopez, “Tuning characteristics, radiation efficiency and subjective quality of a set of classical guitars”, *Appl. Acoust.* **56**, 183–197 (1999).
- ¹⁵ H. Wright, “Acoustics and psychoacoustics of the guitar”, Ph.D. thesis, University of Wales, College of Cardiff, 133–197 (1996).
- ¹⁶ G. Weinreich, “Coupled piano strings”, *J. Acoust. Soc. Am.* **62**(6), 1474–1484 (1977).
- ¹⁷ R. S. Langley, “Spatially averaged frequency response envelopes for one and two-dimensional structural components”, *J. Sound Vib.* **178**(4), 483–500 (1994).
- ¹⁸ E. Skudrzyk, “The mean value method of predicting the dynamic response of complex vibrators”, *J. Acoust. Soc. Am.* **67**(4), 1105–1135 (1980).
- ¹⁹ X. Boutillon and G. Weinreich, “Three-dimensional mechanical admittance : theory and new measurement method applied to the violin bridge”, *J. Acoust. Soc. Am.* **105**(6), 3524–3533 (1999).
- ²⁰ R. Courant and D. Hilbert, *Methods of Mathematical Physics, Volume 1* (Wiley Classic edition, New York, 1989), pp. 429–431.
- ²¹ G. Xie, D. J. Thompson, and C. J. C. Jones, “Mode count and modal density of structural systems : Relationships with boundary conditions”, *J. Sound Vib.* **274**(3), 621–651 (2004).
- ²² J. P. D. Wilkinson, “Modal densities of certain shallow structural elements”, *J. Acoust. Soc. Am.* **43**(2), 245–251 (1968).
- ²³ I. Elishakoff, “Distribution of natural frequencies in certain structural elements”, *J. Acoust. Soc. Am.* **57**(2), 361–369 (1975).
- ²⁴ D. J. Ewins, *Modal Testing* (Research Studies Press, Taunton, 1984), pp. 153–196.
- ²⁵ N. M. M. Maia and J. M. M. Silva, “Modal analysis identification techniques”, *Philos. Trans. R. Soc. London* **359**, 29–40 (2001).
- ²⁶ R. O. Schmidt, “Multiple emitter location and signal parameter estimation”, *IEEE Trans. Antennas Propag.* **34**(3), 276–280 (1986).
- ²⁷ Y. Hua and T. K. Sarkar, “Matrix pencil method for estimating parameters of exponentially damped/undamped sinusoids in noise”, *IEEE Trans. Acoust. Speech Sig. Process.* **38**(5), 814–824 (1990).
- ²⁸ R. Roy and T. Kailath, “Esprit – estimation of signal parameters via rotational invariance techniques”, *IEEE Trans. Acoust. Speech Sig. Process.* **37**(7), 984–995 (1989).
- ²⁹ J.-L. Le Carrou, F. Gautier, N. Dauchez, and J. Gilbert, “Modelling of sympathetic string vibrations”, *Acta. Acust. Acust.* **91**, 277–288 (2005).
- ³⁰ B. David, “Caractérisations acoustiques de structures vibrantes par mise en atmosphère raréfiée (Acoustical characterization of vibrating structures in low atmospheric pressure)”, Ph.D. thesis, Université Pierre and Marie Curie - Paris VI, 170–180 (1999).
- ³¹ R. Badeau, B. David, and G. Richard, “A new perturbation analysis for signal enumeration in rotational invariance techniques”, *IEEE Trans. Sig. Proc.* **54**(2), 450–458 (2006).
- ³² K. Ege, D. Boutillon, and B. David, “High-resolution modal analysis”, *J. Sound Vib.* **325**, 852–869 (2009).
- ³³ J. Laroche, “The use of the matrix pencil method for the spectrum analysis of musical signals”, *J. Acoust. Soc. Am.* **94**(4), 1958–1965 (1993).
- ³⁴ M. Géradin and D. Rixen, *Théorie des vibrations. Application à la dynamique des structures (Theory of vibrations. Application to structural dynamics)* (Editions Masson, Paris, 1992), pp. 119–123.
- ³⁵ G. Bienvenu and L. Kopp, “Optimality of high-resolution array processing using the eigensystem method”, *IEEE Trans. Acoust. Speech Sig. Process.* **31**(5), 1235–1245 (1983).
- ³⁶ M. Wax and T. Kailath, “Detection of signals by information theoretic criteria”, *IEEE Trans. Acoust. Speech Sig. Process.* **33**(2), 387–392 (1985).
- ³⁷ H. Akaike, “Information theory and an extension of the maximum likelihood principle”, in *Proceedings of the 2nd International Symposium on Information Theory, Budapest, Romania*, 267–281 (1973).
- ³⁸ G. Schwarz, “Estimating the dimensions of a model”, *Ann. Stat.* **6**(2), 461–464 (1978).
- ³⁹ M. E. McIntyre and J. Woodhouse, “On measuring the elastic and damping constants of orthotropic sheet materials”, *Acta Metall.* **36**(6), 1397–1416 (1988).
- ⁴⁰ T. Ono, S. Miyakoshi, and U. Watanabe, “Acoustic characteristics of unidirectionally fiber-reinforced polyurethane foam composites for musical instrument soundboards”, *Acoust. Sci. Technol.* **23**(3), 135–142 (2002).